

Patch Antenna with L-Shaped Radiators

Z. Merve Şencan¹ and Ş. Taha İmeci²

¹ Department of Electronics and Communication Engineering
Haliç University, İstanbul, TURKEY
z.m.sencan@hotmail.com

² Department of Electrical and Electronics Engineering
KTO Karatay University, Konya, TURKEY
taha.imeci@karatay.edu.tr

Abstract: This is a microstrip patch antenna paper which conducts parametric study, optimization, and presents simulation results. Simulated results for the center frequency of 5.795 Ghz (IEEE 802.11a) are as follows: very low return loss of – 47.28 dB, theta polarized electric field gain of 7.81 dB, real part of the input impedance as 50.95 ohm, and the imaginary part of the input impedance as – 0.16 ohm. Simulation results are achieved via 3D planar electromagnetic simulation tool, called Sonnet Suites [1].

Keywords: Antenna ,Wireless , Microstrip, Patch, Gain

1. Introduction

There are numerous works about this topic because of the lightweight and easy to fabricate and other advantages of the microstrip patch antennas. Some previous works are also dealing with the geometry of the patch in order to maintain the desired specifications [2]. Another work has a result exactly at the same frequency compared with this project, by using the antenna in low-temperature cofired ceramics (LTCC) packaging modules for wireless applications [3]. They do have relatively low gain due to the high dielectric constant and the thin substrate thickness.

2. Design procedure

The design started with the low gain since the antenna was in a square box even though the geometry, seen on figure 1, is rectangular. After making the box big enough (X=22000 mils, Y=42000 mils), the results were better. Dielectric is Arlon Foam Clad with $\epsilon_r = 1.25$. A random optimization by changing two parameters is conducted and presented in Tables 1 – 5. These are the dielectric thickness and the reference planes/calibration lengths.

Table 1:Ref. = 9000 mils

| Thickness | Gain(dB) (0°) | $Z_{in}(\text{real})(\Omega)$ | $Z_{in}(\text{imaginary})(\Omega)$ | $S_{11}(\text{dB})$ | f_c (Ghz) |
|-----------|---------------|-------------------------------|------------------------------------|---------------------|-------------|
| 30 | 6.89 | 48.37 | -19.23 | -13.36 | 6.45 |
| 60 | 7.61 | 42.7 | 5.88 | -19.64 | 5.71 |
| 80 | 7.61 | 54.6 | 0 | -27 | 5.69 |
| 120 | 6.48 | 75 | 4.72 | -25.25 | 6.88 |

Table 2:Ref. 10000 mils

| Thickness | Gain(dB) $\theta(0^\circ)$ | $Z_{in}(\text{real } \Omega)$ | $Z_{in}(\text{imaginary})(\Omega)$ | $S_{11}(\text{dB})$ | f_c (Ghz) |
|-----------|----------------------------|-------------------------------|------------------------------------|---------------------|-------------|
| 30 | 9.8 | 34.72 | 9.70 | -12.7 | 7.04 |
| 60 | 7.6 | 42.6 | 0.49 | -21.93 | 5.72 |
| 80 | 7.53 | 56 | 2.67 | -22 | 5.71 |
| 120 | 7.15 | 88 | 0 | -11.13 | 5.68 |

Table 3:Ref. 10100 mils

| Thickness | Gain(dB) $\theta(0^\circ)$ | $Z_{in}(\text{real } \Omega)$ | $Z_{in}(\text{imaginary})(\Omega)$ | $S_{11}(\text{dB})$ | f_c (Ghz) |
|-----------|----------------------------|-------------------------------|------------------------------------|---------------------|-------------|
| 30 | 10.03 | 36 | -5 | -15.07 | 7.05 |
| 60 | 7.67 | 44 | 0.38 | -22.81 | 5.76 |
| 80 | 7.35 | 58 | 4.5 | -21.11 | 5.75 |
| 120 | 6.85 | 95 | -3.7 | -10.12 | 5.71 |

Table 4:Ref. 10200 mils

| Thickness | Gain(dB) $\theta(0^\circ)$ | $Z_{in}(\text{real } \Omega)$ | $Z_{in}(\text{imaginary})(\Omega)$ | $S_{11}(\text{dB})$ | f_c (Ghz) |
|-----------|----------------------------|-------------------------------|------------------------------------|---------------------|--------------|
| 30 | 10.28 | 35 | -5 | -14.8 | 7.07 |
| 60 | 8.01 | 38.3 | -2 | -17.38 | 5.8 |
| 80 | 7.84 | 50.95 | -0.16 | -40.377 | 5.795 |
| 120 | 2.26 | 82 | 12 | 82 | 5.78 |

The best result was achieved when cal. length was 10200 mils, as shown on Table 4, in bold.

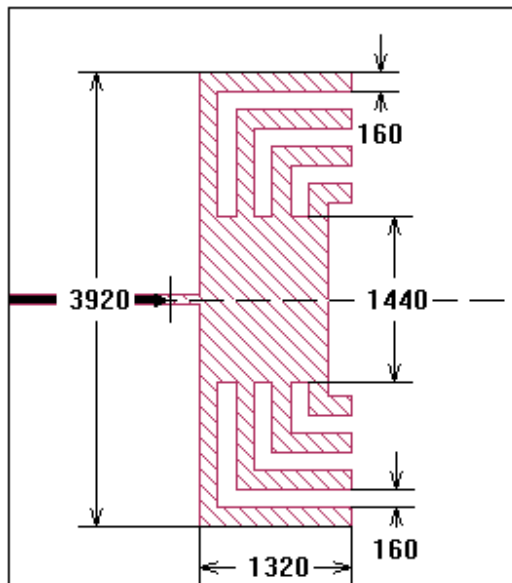


Fig. 1. Top view and dimensions of the antenna (mils).

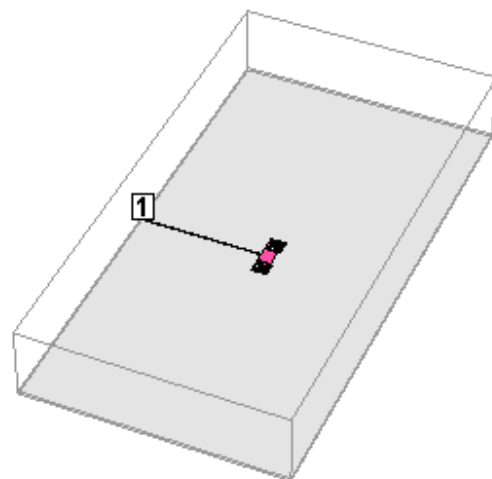


Fig. 2. 3D view of the antenna.

3. Simulation Results

The simulation result of the return loss is shown in Figures have the real part and the imaginary part of Z_{in} . Since the return loss is very low (-47.28 dB), the real part of the input impedance is very close to 50 ohms and the imaginary part is very close to zero.

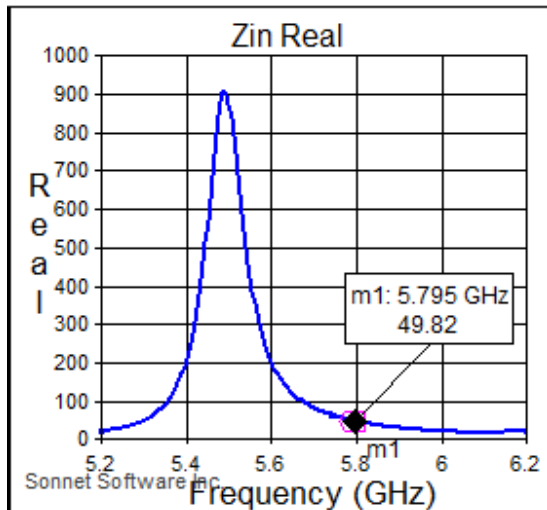


Fig. 3. Input impedance of the antenna.

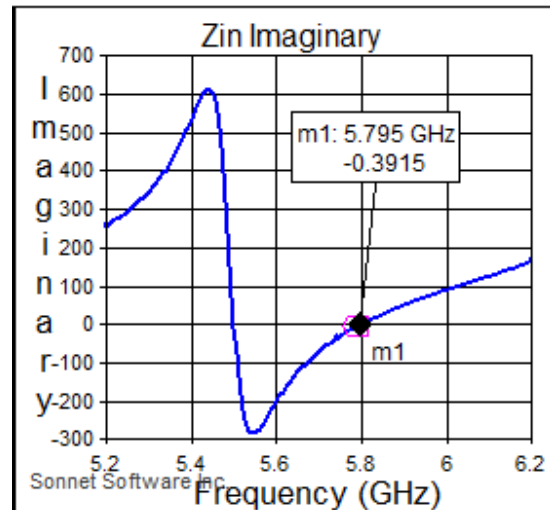


Fig. 4. Imaginary part of the input impedance.

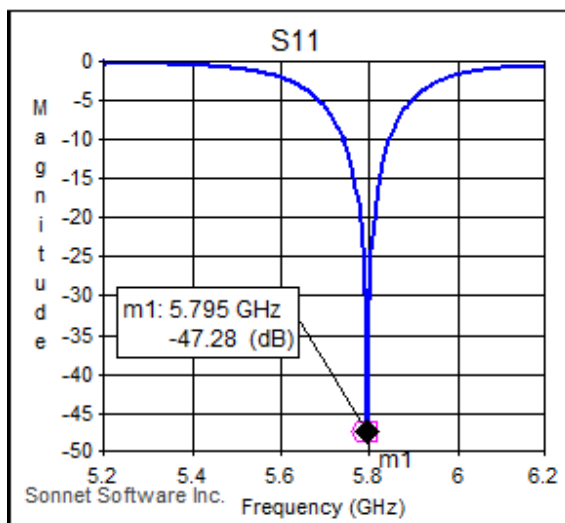


Fig. 5. Return loss of the antenna.

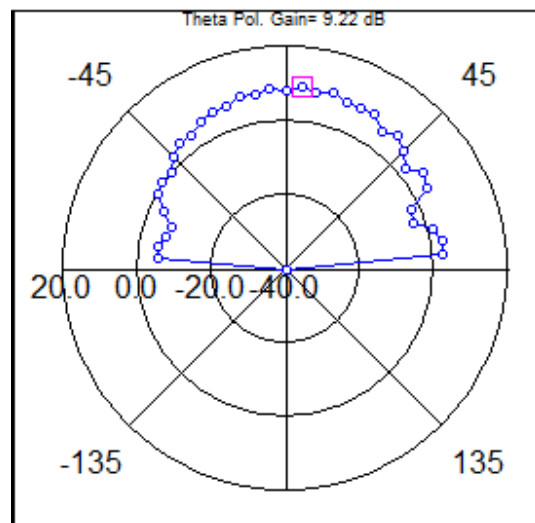


Fig. 6. Radiation pattern of the antenna.

Figure 6 shows the radiation pattern. Cross-pol. level is less than -40 dB. Table 5 show the gain values at different theta degrees for edge-feeding. Higher gain values at different degrees shown in bold

Since the radiation pattern is not smooth and, because of the long edge-feeding line, probe feeding is tried. Figures 7 and 8 have the S11 and radiation pattern with rectangular via feeding. Tables 6 and 7 have parameters with rectangular via feeding.

Table 5: Radiation pattern gain points at different theta values for edge-feeding.

| | | | | | | | | | | |
|---------------------|------|------|------|------|------|------|------|-------------|-------------|-------------|
| $\theta (^{\circ})$ | -50 | -45 | -40 | -35 | -30 | -25 | -20 | -15 | -10 | -5 |
| Gain(dB) | 0.31 | 2.50 | 4.43 | 4.09 | 5.87 | 6.58 | 6.66 | 8.12 | 7.38 | 8.95 |
| $\theta (^{\circ})$ | 50 | 45 | 40 | 35 | 30 | 25 | 20 | 15 | 10 | 5 |
| Gain(dB) | 2.24 | 4.59 | 7.23 | 5.03 | 7.92 | 7.65 | 7.88 | 8.90 | 7.95 | 9.23 |

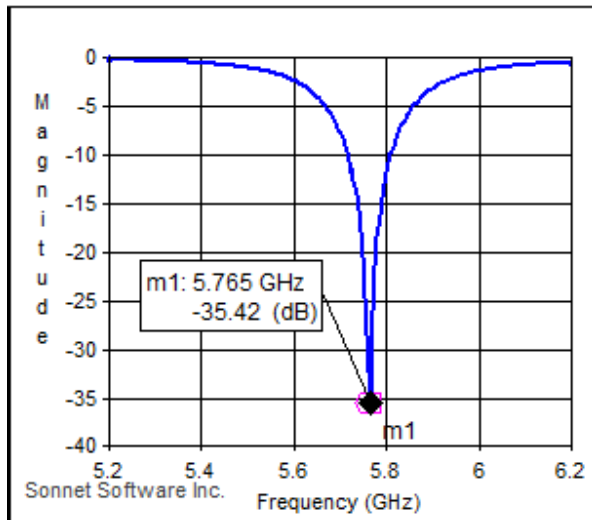


Fig. 7. Return loss of the antenna.

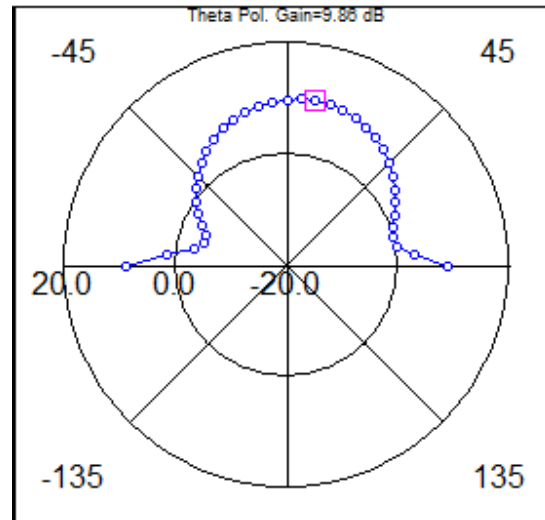


Fig. 8. Radiation Pattern of the antenna.

Table 6: Gain, Z_{in} , S_{11} and f_c values in different rectangular via dimensions.

| Via Attributes (Width,Height) | Gain $\theta(0^{\circ})$ (dB) | Z_{in} (real Ω) | Z_{in} (imag. Ω) | S_{11} (dB) | f_c (Ghz) |
|-------------------------------|-------------------------------|---------------------------|----------------------------|---------------|--------------|
| (20,10) | 9.86 | 50.59 | 1.59 | -35.42 | 5.765 |
| (40,20) | 9.87 | 42.75 | 5.20 | -20.35 | 5.8 |
| (80,40) | 9.92 | 36.9 | -5.5 | -16.23 | 5.82 |
| (120,60) | 9.98 | 32.34 | -8.5 | -11.9 | 5.85 |

Table 7: Radiation pattern gain points at different theta values for edge-feeding.

| | | | | | | | | | | |
|---------------------|------|-----|-----|-----|-----|-----|-----|-----|-----|-----|
| $\theta (^{\circ})$ | -50 | -45 | -40 | -35 | -30 | -25 | -20 | -15 | -10 | -5 |
| Gain(dB) | 1.24 | 2.6 | 3.9 | 5 | 6.1 | 7 | 7.8 | 8.5 | 9 | 9.4 |
| $\theta (^{\circ})$ | 50 | 45 | 40 | 35 | 30 | 25 | 20 | 15 | 10 | 5 |
| Gain(dB) | 4.93 | 6 | 7 | 7.8 | 8.5 | 9 | 9.5 | 9.7 | 9.8 | 9.8 |

Figures 9 and 10 have the S_{11} and radiation pattern with circular via feeding. Tables 8 and 9 have parameters with circular via feeding.

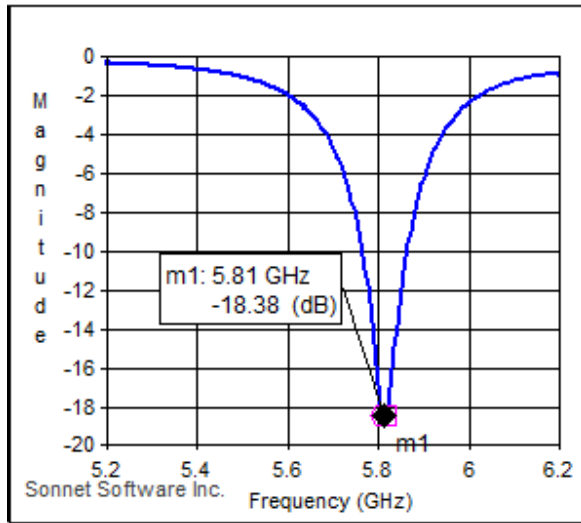


Fig. 9. Return loss of the antenna.

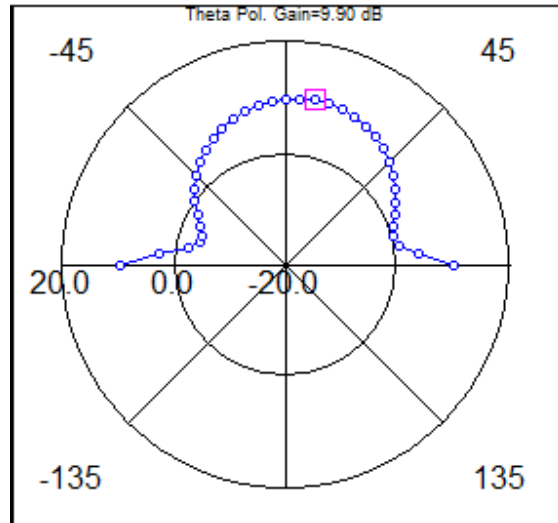


Fig. 10. Radiation Pattern of the antenna.

Table 8: Gain, Z_{in} , S_{11} and f_c values in different circular via dimensions.

| Via Attributes (Diameter, Num. Sides) | Gain $\theta(0^\circ)$ (dB) | Z_{in} (real Ω) | Z_{in} (imag. Ω) | S_{11} (dB) | f_c (Ghz) |
|--|--------------------------------|------------------------------|-------------------------------|------------------|----------------|
| (40,20) | 9.92 | 36.09 | -4.29 | -15.45 | 5.83 |
| (50,25) | 9.90 | 39.45 | -1.87 | -18.37 | 5.81 |
| (60,30) | 9.90 | 39.27 | -3.31 | -18.01 | 5.815 |
| (80,40) | 9.92 | 36 | -4.26 | -15.45 | 5.83 |

Table 9: Radiation pattern gain points at different theta values for edge-feeding.

| | | | | | | | | | | |
|-----------------------|------|-----|-----|-----|-----|-----|-----|------|-----|----|
| θ ($^\circ$) | -50 | -45 | -40 | -35 | -30 | -25 | -20 | -15 | -10 | -5 |
| Gain(dB) | 1.26 | 4.4 | 5.5 | 6.6 | 7.5 | 8.3 | 8.9 | 9.43 | 9.8 | 10 |
| θ ($^\circ$) | 50 | 45 | 40 | 35 | 30 | 25 | 20 | 15 | 10 | 5 |
| Gain(dB) | 5.02 | 4,6 | 5.7 | 6.7 | 7.5 | 8.3 | 8.9 | 9.5 | 9.8 | 10 |

Figures 11 and 12 have the current distribution on the antenna for edge-feeding and with circular via feeding, respectively. Figures clearly show that the current is crowded at the center of the patch since this is a broadside radiated antenna.

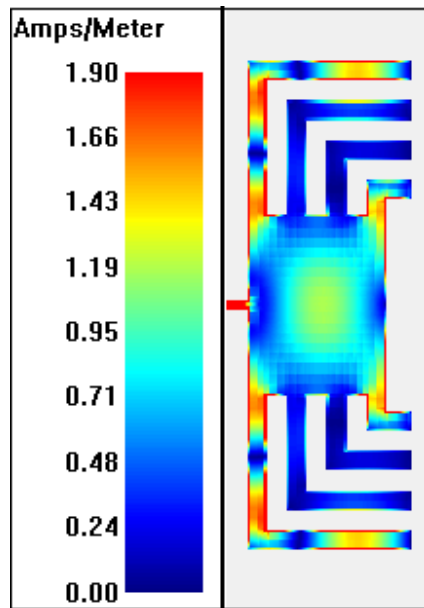


Fig. 11. Current distribution of the antenna with edge-feeding

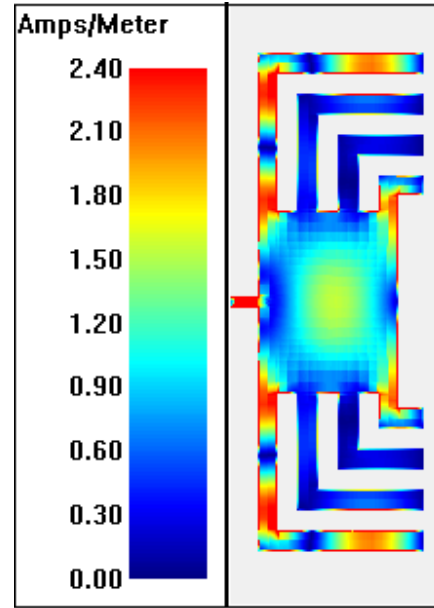


Fig. 12. Current distribution of the antenna with probe-feeding

4. Conclusions

In this work, a microstrip patch antenna is designed and simulated for the IEEE 802.11a band. An optimization by changing the dielectric thickness and the reference planes/calibration lengths is conducted. Simulated results are satisfactory. A very low return loss (-40.377 dB) gave almost ideal input impedance values (real: 50.95Ω and imaginary: -0.16Ω) and a moderate gain (7.81 dB when $\theta = 0^\circ$). 10 dB return loss bandwidth is 1.72%. Another analysis with probe-feeding gave better gain values. Future work is trying to make the radiation pattern more symmetric and fabrication of the antenna.

References

- 1 Sonnet Software, version 12.56, www.sonnetsoftware.com, 2009.
- 2 Ş. T. İmeci, M. A. Kızrak, and İ. Şişman "Circularly Polarized Microstrip Patch Antenna with Slits", *ACES Conference* Tampere, Finland, 2010.
- 3 R. Li, *Senior Member, IEEE*, G. DeJean, M. Maeng, K. Lim, S. Pintel, M. M. Tentzeris, *Senior Member, IEEE*, J. Laskar, *Senior Member, IEEE* "Design of Compact Stacked-Patch Antennas in LTCC Multilayer Packaging Modules for Wireless Applications", *IEEE Transactions on Advanced Packaging*, Vol. 27, No 4, November 2004.
- 4 D. Pan, Chung G. "Optimization of Reconfigurable Inset-Fed Microstrip Patch Antennas with High Gain for Wireless Sensor Networks", July 2009.